

DUET-VLM: Dual stage Unified Efficient Token reduction for VLM Training and Inference

Aditya Kumar Singh*, Hitesh Kandala*, Pratik Prabhanjan Brahma, Zicheng Liu, Emad Barsoum
Advanced Micro Devices, Inc. (AMD)

*Equal contribution

Abstract

Vision-language models (VLMs) have achieved remarkable multimodal understanding and reasoning capabilities, yet remain computationally expensive due to dense visual tokenization. Existing efficiency approaches either merge redundant visual tokens or drop them progressively in language backbone, often trading accuracy for speed. In this work, we propose DUET-VLM, a versatile plug-and-play dual compression framework that consists of (a) vision-only redundancy aware compression of vision encoder’s output into information-preserving tokens, followed by (b) layer-wise, salient text-guided dropping of visual tokens within the language backbone to progressively prune less informative tokens. This coordinated token management enables aggressive compression while retaining critical semantics. On LLaVA-1.5-7B, our approach maintains over 99% of baseline accuracy with 67% fewer tokens ↓, and still retains >97% even at 89% ↓ reduction. With this dual-stage compression during training, it achieves 99.7% accuracy at 67% ↓ and 97.6% at 89% ↓, surpassing prior SoTA visual token reduction methods across multiple benchmarks. When integrated into Video-LLaVA-7B, it even surpasses the baseline—achieving >100% ↑ accuracy with a substantial 53.1% ↓ token reduction and retaining 97.6% accuracy under an extreme 93.4% ↓ setting. These results highlight end-to-end training with DUET-VLM, enabling robust adaptation to reduced visual (image/video) input without sacrificing accuracy, producing compact yet semantically rich representations within the same computational budget. Our code is available at <https://github.com/AMD-AGI/DUET-VLM>.

1. Introduction

In the realm of multimodal intelligence, *an image is worth a thousand words* but also thousands of tokens. Each image encodes colors, textures, and spatial cues that enrich linguistic reasoning, yet this expressivity burdens vision-language models (VLMs) with an overwhelming number of visual

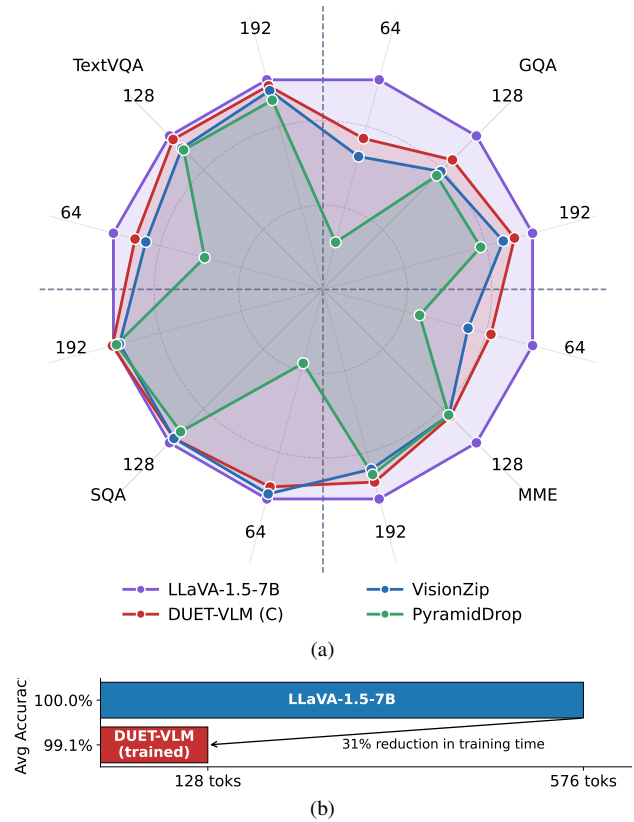


Figure 1. **Efficiency and accuracy comparison of DUET-VLM.** (a) shows the average inference-only accuracy of VisionZip, PyramidDrop, and DUET-VLM across different token budgets, compared to the full 576-token LLaVA-1.5-7B baseline on four benchmarks. (b) demonstrates that trained DUET-VLM model achieves a 31% reduction in training time while incurring less than a 1% drop in accuracy relative to the LLaVA-1.5-7B baseline.

with image resolution ($H \times W$), compounding the already quadratic attention cost and making large vision-language models (LVLMs) both memory- and latency-bound.

Recent studies [16, 21, 33] confirm that scaling up visual tokens boosts grounding and reasoning accuracy. Yet, this improvement comes at a high computational cost, motivating a surge of research into efficient visual compression.

Two primary fronts for multimodal efficiency are (i) *vision-side* and (ii) *language-side* compression, each targeting redundant visual computation and quadratic attention costs. (i) Methods in this category aim to compact the visual embedding space even before cross-modal interaction [1, 23, 30]. Whereas (ii) prune redundant visual tokens *during or after* their interaction with the language model [5, 28, 31].

Our Perspective. In summary, existing methods either (a) *merge too early*, risking information loss (VisionZip [30], PruMerge [23]), or (b) *drop too uniformly*, lacking semantic adaptivity (PyramidDrop [28], FitPrune [31]). Others (FastV [5], HiRED [1]) offer partial adaptivity but remain *single directional*, compressing only once, either before or during reasoning, thus failing to jointly optimize *redundancy removal* and *context-aware retention*.

Our Approach. In this paper, we introduce DUET-VLM, a *unified two-way visual compression framework* that jointly optimizes redundancy removal and contextual adaptivity across the vision-language interface. DUET-VLM operates in two complementary stages: (1) *Vision-to-Vision (V2V) merging*, which merges correlated patches into compact embeddings, reducing redundancy before cross-modal fusion; and (2) *Text-to-Vision (T2V) pruning*, which dynamically prunes visual tokens at successive layers using text-to-vision attention scores. This dual-stage design, coupling early *structural merging* with late *semantic pruning*, retains essential low-level visual details for grounding early on while progressively removing redundant tokens as reasoning deepens. As a consequence, it maintains near-baseline accuracy even under extreme token compression, preserving over 99% of baseline-performance at 67% token reduction and above 97% at 89% reduction during inference across multiple image benchmarks, as shown in Fig. 1. This trend extends to video understanding as well, where our method surpasses the baseline ($>100\%$ accuracy) with 53.1% token reduction and still achieves 97.6% accuracy under an extreme 93.4% reduction. These results show that smart token compression can match or even surpass traditional scaling.

In summary, our contributions are:

- **Joint Vision–Language Optimization:** Unlike prior one-sided compression schemes, we couple both the vision and language backbones through a differentiable compression interface, enabling visual representations and linguistic context to co-adapt during token reduction while maintaining strong cross-modal alignment and efficiency.

- **Dual-Stage Visual Compression:** A unified, task-agnostic framework (DUET-VLM) that first performs *redundancy-aware visual token merging* into compact, information-preserving tokens, followed by *layer-wise saliency-based text-guided token dropping* within language counterpart to prune less informative tokens.

- **Accuracy Retention:** DUET-VLM preserves semantic richness and cross-modal reasoning, maintaining over 99% of baseline accuracy with only one-third of the original visual tokens across multiple image and video benchmarks.

Overall, DUET-VLM shows that careful token management can match model scaling in accuracy while significantly reducing compute.

2. Related Works

Token Efficiency in VLMs. The rise of LLMs [2, 6, 7, 20, 22, 27, 35] has driven the development of large vision-language models (LVLMs) [4, 8, 14, 16, 26, 36], which align visual encoders such as CLIP [21] or SigLIP [33] with powerful text decoders for unified multimodal reasoning. However, high-resolution vision inputs yield hundreds to thousands of tokens (e.g., 672×672 images producing $> 2,800$ tokens in LLaVA-NeXT [18]), causing quadratic growth in transformer attention cost. This has led to a spectrum of token-efficiency methods, majorly drawing inspiration from token reduction in LLMs [11, 25]. We broadly categorized these methods as *vision-encoder-side compression* and *language-side compression*. The former class targets redundancy at the feature-extraction stage: VisionZip [30] merges visually similar patches into representative tokens while retaining irreducible dominant ones, HiRED [1] uses CLS-guided saliency to allocate a fixed token budget across high-resolution partitions, and PruMerge [23] merges unpruned tokens via attention-sparsity clustering. These approaches effectively reduce visual clutter before multimodal fusion, but their static or heuristic merging strategies limit downstream adaptivity. In contrast, language-side compression techniques such as PyramidDrop [28] progressively drop visual tokens across transformer layers, FastV [5] learns adaptive attention masks to prune tokens in deeper stages, and FitPrune [31] devises a training-free pruning recipe matching pre- and post-pruning attention distributions. While these methods achieve substantial FLOP savings, they operate within a single stage either compressing early or pruning late thus lacking synergy between the vision and language representations.

Joint Multimodal Compression. Recent studies suggest that redundancy evolves across both spatial and semantic hierarchies [28, 30], motivating approaches that reason jointly over vision and text-conditioned saliency. Our work builds upon this insight, extending VisionZip’s early-stage merging and PyramidDrop’s progressive pruning under a unified,

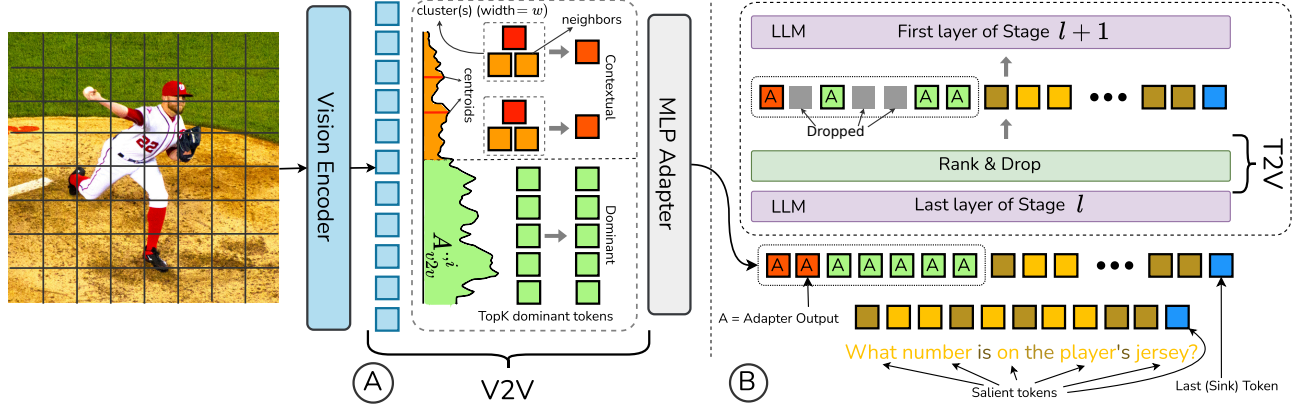


Figure 2. **Overview of the proposed pipeline.** An input image is first encoded into N visual tokens by the *Vision Encoder*. (A) Based on the V2V self-attention map $A_{v2v}^{j,i} := 1/N \sum_j A_{v2v}^{j,i}$, we select the most influential Top- k_1 *dominant tokens*, while the remaining tokens, \mathbf{X}_{res} , are merged into k_2 *contextual tokens* via attention-guided clustering with a fixed cluster width w , to reduce redundancy. (B) The resulting reduced visual tokens, \mathbf{X}_{out} , are fed into a language backbone after projecting it through an *MLP Adapter*, where salient text tokens, S , further prune visual tokens based on cross-attention scores A_{t2v} at certain selected layers called *stages*.

differentiable framework. Unlike these prior methods, we merge fewer yet contextually coherent tokens per cluster in the vision encoder, preserving structural diversity, and incorporate salient text-guided tokens for layer-wise adaptive dropping in the LLM. This coupling of vision-side compaction with language-guided pruning achieves joint optimization under a fixed token budget, yielding higher accuracy than existing single-stage compressors across multiple multimodal benchmarks. A detailed formulation of this dual-stage pipeline linking redundancy-aware merging and saliency-driven pruning is presented next in our Sec. 3.

3. Methodology

Our approach primarily combines VisionZip’s [30] visual token reduction followed by PyramidDrop’s [28] hierarchical text-based visual tokens pruning. VisionZip reduces all visual tokens to (a) dominant tokens and (b) contextual tokens, where we modify contextual token construction via our novel approach of local cluster aggregation as formalised in Secs. 3.1 and 3.1.1 and Fig. 2(A). For PyramidDrop, instead of last text token, we experiment with various salient token selection methods as shown in Sec. 3.2 and further experimented in Tabs. 8 and 9.

3.1. Clustering of vision tokens

Let $\mathbf{X} := \{\mathbf{x}_i\}_{i=1}^N \in \mathbb{R}^{N \times d}$ denote the set of N vision tokens from the vision encoder, with d being the embedding dimension. With help of self-attention map $A_{v2v} \in \mathbb{R}^{N \times N}$ retrieved from CLIP’s last layer, we further identify a subset of k_1 dominant tokens, \mathbf{X}_{dom} , that has high vision-to-vision affinity, where $|\mathbf{X}_{\text{dom}}| = k_1 < N$. For residual vision tokens, we merge them into k_2 tokens via clustering, as shown in Algo. 1.

Algorithm 1 Attention guided Dominant selection + Residual Clustering

- Require:** Tokens $\mathbf{X} = \{\mathbf{x}_i\}_{i=1}^N$, attention map $A_{v2v} \in \mathbb{R}^{N \times N}$, k_1, k_2, w (= cluster-size)
- Ensure:** Reduced tokens $\mathbf{X}_{\text{out}} = \mathbf{X}_{\text{dom}} \cup \mathbf{X}_{\text{comp}}$, where \mathbf{X}_{comp} = contextual tokens
- 1: Functions: $\text{TopK}()$ takes two arguments, (i) an array and (ii) size of set of top elements in the array to be selected.
 - 2: Compute attention score $s_i = \sum_{j=1}^N A_{v2v}^{j,i}$, select dominant indices $\mathcal{D} := \text{TopK}(\{s_i\}, k_1)$ and residual indices $\mathcal{R} := \{1, \dots, N\} \setminus \mathcal{D}$.
 - 3: From \mathcal{R} , pick cluster centroids

$$\mathcal{C} := \text{TopK}(\{s_i\}_{i \in \mathcal{R}}, k_2) \quad (1)$$
 - 4: For each centroid $c \in \mathcal{C}$, get neighbors’ indices

$$\mathcal{N}_c = \text{TopK}(A_{v2v}^{c, \mathcal{R}}, w) \quad (2)$$
 and form $\mathbf{z}_c = \sum_{j \in \mathcal{N}_c} \mathbf{x}_j / |\mathcal{N}_c|$.
 - 5: Return $\mathbf{X}_{\text{dom}} = \{\mathbf{x}_i\}_{i \in \mathcal{D}}$ and $\mathbf{X}_{\text{comp}} = \{\mathbf{z}_c\}_{c \in \mathcal{C}}$, *i.e.* $\mathbf{X}_{\text{out}} = \mathbf{X}_{\text{dom}} \cup \mathbf{X}_{\text{comp}}$.
-

3.1.1. Motivation for local clustering

a. Semantic misalignment. The dominant tokens often correspond to high-activation visual areas which might not be semantically relevant for downstream text-guided tasks.

b. Information dilution. When the volume of residual tokens is large, *i.e.* $|\mathbf{X}_{\text{res}}| \gg k_2$, where $\mathbf{X}_{\text{res}} := \mathbf{X} \setminus \mathbf{X}_{\text{dom}}$ all visual tokens except k_1 dominant tokens, averaging dilutes the semantically informative but low-frequency features.

Local Cluster Aggregation. To address these limitations,

we replace global averaging with *local cluster aggregation*. Instead of merging all non-dominant tokens into a few global contextual vectors, we partition the residual tokens \mathbf{X}_{res} into k_2 small clusters with centroid c and their neighbors $\{\mathcal{N}_c\}_{c \in \mathcal{C}}$ where each cluster produces one contextual token via local averaging. We choose centroids based on the ranking of V2V self-attention scores (A_{v2v}) to have a good basis for forming the context. Importantly, we do *not* increase the number of contextual tokens; instead, we maintain k_2 , while enforcing a small cluster width w , where $w = |\mathcal{N}_c|$. This has two advantages: (a) *Aggregation* is performed within a local neighborhood \mathcal{N}_c , preserving fine-grained cues while avoiding dilution by background noise. (b) Since $w \cdot k_2 < |\mathbf{X}_{\text{res}}|$, the unassigned tokens in \mathbf{X}_{res} are *dropped* early, effectively removed from the pipeline before entering the language backbone. For example, with $N=576$, $k_1=54$, $k_2=10$, and $w=4$, a total of $576 - 54 - (10 \cdot 4) = 482$ tokens are dropped before reaching the language backbone.

3.2. Hierarchical visual tokens dropping

For LLM, we wrap the compact set of visual tokens with textual tokens, *i.e.*, a *system prompt* at the beginning and *query* tokens at the end.

Let $\mathcal{T} := \{t_k\}_{k=1}^m$ be the full sequence of text tokens (queries). Importantly, while the entire text sequence \mathcal{T} is preserved and passed through the network, only a subset of salient text tokens, \mathcal{S} identified by the salient-token estimator $F_S(\cdot)$, is used to compute text-to-vision (T2V) saliency, which then forms the basis for progressive visual token pruning across the language layers. The last text token (t_m) is always included in \mathcal{S} as a *sink* token to stabilize the attention and capture globally relevant prompt-context as well as visually critical regions even under aggressive pruning [28].

Text-Guided Visual Token Dropping. Let us assume we have L layers in the language backbone, grouped into M stages with $M < L$. We define $\mathcal{V}^{(l)}$ to be set of visual tokens retained at stage $l \in \{1, \dots, M\}$ with $N_l := |\mathcal{V}^{(l)}|$. And for $l = 0$, we have $\mathcal{V}^{(0)} = \mathbf{X}_{\text{out}}$ and $N_0 = |\mathbf{X}_{\text{out}}| = k_1 + k_2$ visual tokens. Now, given a target compression ratio λ , after each stage l , we drop $\lfloor \lambda \cdot N_l \rfloor$ or retain $\lfloor (1 - \lambda) \cdot N_l \rfloor$ tokens based on T2V cross-attention scores $A_{t2v}^{(l)} \in \mathbb{R}^{|\mathcal{S}| \times N_l}$ between the salient text tokens \mathcal{S} and retained vision tokens $\mathcal{V}^{(l)}$, as shown in Fig. 2(B). First, we rank visual tokens ($\mathcal{V}^{(l)}$) in descending order and then we choose first $\lfloor (1 - \lambda) \cdot N_l \rfloor$ tokens, essentially doing $\text{TopK}(\mathcal{V}^{(l)}, \lfloor (1 - \lambda) \cdot N_l \rfloor)$. This rank-and-drop procedure is repeated at each stage, progressively narrowing the visual context by filtering redundant visual information as multimodal reasoning deepens. This enforces an adaptive balance between computational efficiency and representational fidelity and ensures that higher layers attend only to semantically relevant regions.

4. Experiment

4.1. Setup

Implementation Details. We evaluate our method across three settings. For image-based tasks, we use LLaVA-1.5-7B [17] with 576 vision tokens from the vision encoder. For inference-only comparisons, we include LLaVA-NeXT-7B [18], which supports 2,880 vision tokens. Training experiments are conducted on LLaVA-1.5-7B, while for video understanding tasks we use Video-LLaVA-7B [15], which processes 8 frames per video with up to 2,048 vision tokens. Unless otherwise specified, we adopt a default cluster width of 4 and an LLM configuration $\{\text{layer: token-retention-ratio}\} = \{16:0.5, 24:0\}$, indicating that 50% of the tokens are retained after the 16th layer, while all remaining tokens are dropped after the 24th layer. This configuration is chosen to balance mid-layer contextualization with late-layer sparsity, consistent with prior findings [28] that deeper layers contribute less to token-level reasoning. Consistent with these findings, our experiments show that pruning tokens entirely in the final layers (*e.g.*, after the 24th) yields performance nearly identical to retaining them, suggesting that late-stage pruning does not harm multimodal understanding. Please refer to the supplemental for detailed ablations supporting this choice. All experiments were conducted on *one node* of a compute cluster equipped with $8 \times$ AMD Instinct[™] MI325 GPUs. We evaluate four variants of our model throughout the paper:

- DUET-VLM (vanilla): Baseline combining VisionZip-style clustering with the original PyramidDrop strategy, where the *last text token* is used to rank and prune visual tokens within the LLM stages.
- DUET-VLM (C): Variant employing our *local clustering* mechanism in place of VisionZip’s method, still guided by the *last text token* for visual token pruning.
- DUET-VLM (C+all): Extension using local clustering with attention-guided pruning from *all text tokens* for ranking and dropping visual tokens.
- DUET-VLM (C+S): Full model variant combining local clustering with again attention-guided pruning but by the *salient text tokens*, yielding the strongest semantic alignment between vision and language.

Benchmarks. We conduct extensive evaluations on both image and video understanding benchmarks to assess the effectiveness of our approach. For image-based tasks, we benchmark our model on POPE [13], GQA [9], TextVQA (VQA^T) [24], MME [32], SQA-Image (SQA^I) [19], and SeedBench-Image (Seed^I) [12]. For video, we follow the evaluation protocol proposed in Video-LLaVA [15] and evaluate on three widely used video question answering datasets: TGIF-QA [10], MSVD-QA [29], and MSRVTT-QA [29], ensuring consistency and comparability with recent multimodal instruction-tuned models. For all reported tables, we

Table 1. **Comparison of inference-only methods on LLaVA-1.5-7B.** We report results across five benchmarks under different average token budgets, corresponding to 67%, 78%, and 89% token reduction. DUET-VLM (C) achieves the highest average performance across all settings, maintaining over 99% of the baseline accuracy while using significantly fewer tokens.

Method	POPE	SQA ^I	VQA ^T	MME	GQA	Avg
Total 576 Tokens (100.0%)						
LLaVA-1.5-7B	85.9 (100.0%)	69.5 (100.0%)	58.2 (100.0%)	1862 (100.0%)	61.9 (100.0%)	100.0%
Avg 192 Tokens (↓ 66.7%)						
FastV [5] [ECCV'24]	64.8 (75.4%)	67.3 (96.8%)	52.5 (90.2%)	1612 (86.6%)	52.7 (85.1%)	86.8%
HiRED [1] [AAAI'25]	82.8 (96.4%)	68.4 (98.4%)	47.4 (81.4%)	1737 (93.3%)	58.7 (94.8%)	92.9%
FitPrune [31] [AAAI'25]	83.4 (97.1%)	67.8 (97.6%)	57.4 (98.6%)	1831 (98.3%)	60.4 (97.6%)	97.8%
PruMerge [23] [ICCV'25]	71.3 (83.0%)	67.9 (97.7%)	54.3 (93.3%)	1632 (87.6%)	54.3 (87.7%)	89.9%
SparseVLM [34] [ICML'25]	83.6 (97.3%)	69.1 (99.4%)	56.1 (96.4%)	1721 (92.4%)	57.6 (93.1%)	95.7%
PyramidDrop [28] [CVPR'25]	- (-)	69.2 (99.6%)	56.5 (97.1%)	1797 (96.5%)	57.3 (92.6%)	96.4%
VisionZip [30] [CVPR'25]	85.3 (99.3%)	68.9 (99.1%)	57.3 (98.5%)	1783 (95.8%)	59.3 (95.8%)	97.7%
DUET-VLM (C)	86.5 (100.7%)	69.6 (100.1%)	57.7 (99.1%)	1817 (97.6%)	60.3 (97.4%)	99.0%
Avg 128 Tokens (↓ 77.8%)						
FastV [5][ECCV'24]	59.6 (69.4%)	60.2 (86.6%)	52.5 (90.2%)	1490 (80.0%)	49.6 (80.1%)	81.3%
HiRED [1][AAAI'25]	79.8 (92.9%)	68.1 (98.0%)	46.1 (79.2%)	1710 (91.8%)	57.2 (92.4%)	90.9%
FitPrune [31][AAAI'25]	77.9 (90.7%)	68.0 (97.8%)	55.7 (95.7%)	1776 (95.4%)	<u>58.5 (94.5%)</u>	94.8%
PruMerge [23] [ICCV'25]	67.2 (78.2%)	67.1 (96.5%)	54.3 (93.3%)	1554 (83.5%)	53.3 (86.1%)	87.5%
SparseVLM [34] [ICML'25]	80.5 (93.7%)	68.4 (98.4%)	54.9 (94.3%)	1696 (91.1%)	56.0 (90.5%)	93.6%
PyramidDrop [28] [CVPR'25]	- (-)	68.4 (98.4%)	56.6 (97.3%)	1761 (94.6%)	57.1 (92.2%)	95.6%
VisionZip [30] [CVPR'25]	83.2 (96.9%)	68.9 (99.1%)	56.8 (97.6%)	1762 (94.6%)	57.6 (93.1%)	96.3%
DUET-VLM (C)	85.9 (100.0%)	70.2 (101.0%)	57.8 (99.3%)	1767 (94.9%)	59.0 (95.3%)	98.1%
Avg 64 Tokens (↓ 88.9%)						
FastV [5][ECCV'24]	48.0 (55.9%)	51.1 (73.5%)	47.8 (82.1%)	1256 (67.5%)	46.1 (74.5%)	70.7%
HiRED [1][AAAI'25]	73.6 (85.7%)	68.2 (98.1%)	44.2 (75.9%)	1599 (85.9%)	54.6 (88.2%)	86.8%
FitPrune [31][AAAI'25]	60.9 (70.9%)	68.0 (97.8%)	51.2 (88.0%)	1556 (83.6%)	52.3 (84.5%)	85.0%
PruMerge [23] [ICCV'25]	65.3 (76.0%)	68.1 (98.0%)	54.0 (92.8%)	1549 (83.2%)	51.9 (83.8%)	86.8%
SparseVLM [34] [ICML'25]	75.1 (87.4%)	62.2 (89.5%)	51.8 (89.0%)	1505 (80.8%)	52.7 (85.1%)	86.4%
PyramidDrop [28] [CVPR'25]	- (-)	69.0 (99.3%)	50.6 (86.9%)	1561 (83.8%)	47.5 (76.7%)	86.7%
VisionZip [30] [CVPR'25]	77.0 (89.6%)	69.0 (99.3%)	55.5 (95.4%)	1690 (90.8%)	55.1 (89.0%)	92.8%
DUET-VLM (C)	82.5 (96.0%)	68.3 (98.3%)	56.4 (96.9%)	1751 (94.0%)	56.7 (91.6%)	95.4%

compute the percentage performance relative to the baseline for each benchmark and then average these normalized values across all tasks to obtain the Average (Avg.)%, the last column, thus forming a unified metric for comparison across rows.

4.2. Results

Inference-Only Results on LLaVA-1.5-7B. Table 1 compares DUET-VLM against recent inference-only compression/pruning methods on LLaVA-1.5-7B across five standard benchmarks (POPE, SQA, TextVQA, MME, and GQA). The baseline uses 576 visual tokens, while compressed settings use 192, 128, and 64 tokens (67%, 78%, and 89% token reduction). Across all budgets as shown in table 6, DUET-VLM achieves the strongest accuracy–efficiency trade-off, retaining 99.0%, 98.1%, and 95.4% of baseline average accuracy at 192, 128, and 64 tokens, respectively, outperforming

prior methods including FitPrune [31], SparseVLM [34], VisionZip [30], and PyramidDrop [28]. At the matched 192-token setting, DUET-VLM reaches 99.0% relative average accuracy with $1.11\times$ speedup, improving over VisionZip (97.7%, $1.14\times$) and PyramidDrop (96.4%, $0.97\times$); under aggressive compression (64 tokens), it still maintains 95.4% with the highest speedup ($1.16\times$). Notably, at moderate compression, DUET-VLM can even surpass baseline performance on POPE and SQA, suggesting improved robustness under token reduction. Overall, these results indicate that the proposed dual-stage reduction strategy preserves the most informative visual/textual tokens and sustains strong cross-modal reasoning as token budgets shrink. For fairness, the reported results for PyramidDrop are taken directly from their paper, as the authors did not disclose the configuration required to match the average token budgets of 192, 128, and 64 tokens. Additionally, since PyramidDrop does not report

Table 2. **Comparison of inference-only methods on Qwen-2.5-VL-7B.** We report results across five benchmarks under different average token budgets. DUET-VLM (C) achieves the highest average performance across all settings, maintaining over 98% of the baseline accuracy while using significantly fewer tokens.

Method	Speedup	POPE	SQA ^I	VQA ^T	MME	GQA	Avg
Dynamic Tokens							
Qwen-2.5-VL-7B [3]	1.00×	87.8 (100.0%)	86.2 (100.0%)	72.3 (100.0%)	2264 (100.0%)	58.3 (100.0%)	100.0%
Avg 640 Tokens							
VisionZip	1.3x	87.8 (100.0%)	86.2 (100.0%)	71.2 (98.5%)	2267 (100.1%)	58.3 (100.0%)	99.7%
DUET-VLM (C)	1.3x	88.3 (100.6%)	85.8 (99.5%)	71.5 (98.9%)	2264 (100.0%)	58.5 (100.3%)	99.9%
Avg 320 Tokens							
VisionZip	1.4x	88.0 (100.2%)	86.2 (100.0%)	69.4 (96.0%)	2251 (99.4%)	58.2 (99.8%)	99.1%
DUET-VLM (C)	1.4x	88.3 (100.6%)	85.8 (99.5%)	71.3 (98.6%)	2259 (99.8%)	58.5 (100.3%)	99.8%
Avg 160 Tokens							
VisionZip	1.5x	87.4 (99.5%)	86.1 (99.9%)	64.6 (89.3%)	2210 (97.6%)	57.3 (98.3%)	96.9%
DUET-VLM (C)	1.5x	88.2 (100.5%)	86.0 (99.8%)	67.7 (93.6%)	2235 (98.7%)	57.9 (99.3%)	98.4%

Table 3. **Comparison of trained methods on LLaVA-1.5-7B.** We report scores across multiple benchmarks under different visual token budgets. DUET-VLM variants (C), (C+all), and (C+S) defined in Sec. 4.1 consistently outperform or match prior compression approaches such as PyramidDrop and VisionZip, even with reductions of up to 88.9% in visual tokens. These results highlight the effectiveness of training of our dual-stage token selection strategy in preserving baseline accuracy under aggressive compression.

Method	POPE	SQA ^I	VQA ^T	MME	GQA	Avg
Total 576 Tokens						
LLaVA-1.5-7B [17]	85.9 (100.0%)	69.5 (100.0%)	58.2 (100.0%)	1862.0 (100.0%)	61.9 (100.0%)	100.0%
Avg 192 Tokens (↓ 66.7%)						
VisionZip	84.9 (98.8%)	68.2 (98.1%)	57.8 (99.3%)	1834 (98.5%)	60.1 (97.1%)	98.4%
DUET-VLM (C)	85.5 (99.5%)	69.6 (100.1%)	<u>58.2 (100.0%)</u>	1826 (98.1%)	62.4 (100.8%)	99.7%
DUET-VLM (C+all)	85.4 (99.4%)	69.6 (100.1%)	57.7 (99.1%)	1790 (96.1%)	57.6 (93.1%)	97.6%
DUET-VLM (C+S)	85.5 (99.5%)	69.8 (100.4%)	58.5 (100.5%)	1820 (97.7%)	57.6 (93.1%)	98.3%
Avg 128 Tokens (↓ 77.8%)						
VisionZip	83.4 (97.1%)	<u>68.5 (98.6%)</u>	57.1 (98.1%)	1748 (93.9%)	57.6 (93.1%)	96.1%
DUET-VLM (C)	<u>85.1 (99.1%)</u>	<u>68.5 (98.6%)</u>	58.4 (100.3%)	1817 (97.6%)	<u>61.9 (100.0%)</u>	99.1%
DUET-VLM (C+all)	85.4 (99.4%)	67.6 (97.3%)	58.4 (100.3%)	1760 (94.5%)	60.2 (97.3%)	97.8%
DUET-VLM (C+S)	<u>85.1 (99.1%)</u>	69.3 (99.7%)	<u>58.1 (99.8%)</u>	<u>1815 (97.5%)</u>	60.1 (97.1%)	<u>98.6%</u>
Avg 64 Tokens (↓ 88.9%)						
VisionZip	80.9 (94.2%)	68.8 (99.0%)	56.0 (96.2%)	1756 (94.3%)	57.0 (92.1%)	95.2%
DUET-VLM (C)	<u>83.7 (97.4%)</u>	<u>69.5 (100.0%)</u>	<u>57.2 (98.3%)</u>	1737 (93.3%)	<u>60.0 (96.9%)</u>	<u>97.2%</u>
DUET-VLM (C+all)	83.8 (97.6%)	68.0 (97.8%)	57.6 (99.0%)	1736 (93.2%)	57.6 (93.1%)	96.1%
DUET-VLM (C+S)	81.9 (95.3%)	69.8 (100.4%)	57.1 (98.1%)	<u>1754 (94.2%)</u>	61.8 (99.8%)	97.6%

results on the POPE benchmark, the average performance (Avg.) for this method is computed by averaging across the remaining benchmarks to ensure consistent comparison.

Inference-Only Results on Qwen-2.5-VL-7B. Table 2 extends our inference-only evaluation to Qwen-2.5-VL-7B, a more recent VLM architecture, and shows that DUET-VLM generalizes effectively beyond LLaVA-style backbones. Starting from the dynamic-token baseline, both Vi-

sionZip and DUET-VLM (C) provide speedups as token budgets decrease (about 1.3×, 1.4×, and 1.5× at 640, 320, and 160 average tokens), but DUET-VLM (C) consistently preserves higher task performance. In terms of relative average accuracy, DUET-VLM (C) retains 99.9%, 99.8%, and 98.4% across the three budgets, compared with 99.7%, 99.1%, and 96.9% for VisionZip, with the largest margin under the most aggressive compression. DUET-VLM (C) also

Table 4. **Comparison of different methods on Video-LLaVA-7B.** We evaluate performance across three benchmarks to demonstrate that DUET-VLM preserves accuracy even under substantial token compression.

Method	TGIF	MSVD	MSRVTT	Avg
Upper Bound, 2048 Tokens (100%)				
Video-LLaVA	47.1	69.8	56.7	100.0%
Avg 960 Tokens (↓ 53.12%)				
PyramidDrop	46.9	70.0	58.0	100.7%
DUET-VLM (C)	48.9	70.1	55.6	100.8%
Avg 136 Tokens (↓ 93.4%)				
FastV	23.1	38.0	19.3	45.8%
SparseVLM	44.7	68.2	31.0	82.4%
VisionZip	42.4	63.5	52.1	91.0%
DUET-VLM (C)	46.3	67.7	55.2	97.6%

Table 5. **Inference-only speedup comparison on LLaVA-1.5-7B.** DUET-VLM (C) achieves a strong accuracy-latency trade-off under reduced token budgets.

Method	Tokens	Speedup	Avg
LLaVA-1.5-7B	576 (100%)	1x	100.0%
VisionZip	192 (33%)	1.1x	97.7%
PyramidDrop	192 (33%)	1x	96.4%
DUET-VLM (C)	192 (33%)	1.1x	99.0%
DUET-VLM (C)	64 (11%)	1.2x	95.4%

Table 6. **Training time comparison on LLaVA-1.5-7B.** DUET-VLM (C) offers favorable accuracy-efficiency trade-offs with over 30% reduction in training time while still maintaining over 99% accuracy.

Method	Tokens	Train Time ↓	Avg
LLaVA-1.5-7B	576	0%	100.0%
DUET-VLM (C)	192	26%	99.7%
DUET-VLM (C)	128	31%	99.1%
DUET-VLM (C)	64	36%	95.4%

remains stronger on challenging metrics such as TextVQA and GQA at lower token budgets, indicating better preservation of informative visual tokens under heavy compression. Overall, these results confirm that DUET is not only effective on earlier architectures, but also robust on recent models such as Qwen-2.5-VL-7B.

Training Results on LLaVA-1.5-7B. Table 3 presents the comparison of trained methods under different token budgets. Our proposed model variants are compared against VisionZip and PyramidDrop using average token counts of

192, 128, and 64, corresponding to 67%, 78%, and 89% token reduction, respectively. Across all compression levels, DUET-VLM consistently achieves superior or comparable performance. At 192 tokens, DUET-VLM (C) attains an average accuracy of 99.7%, closely matching the full-token LLaVA baseline, and even surpasses it on benchmarks such as POPE [13] and GQA [9]. As the token budget decreases, our method retains performance more effectively than VisionZip, highlighting the benefit of dual-stage compression. All three variants perform competitively, with (C+S) slightly outperforming others at lower token budgets.

Table 6 further summarizes the training-time trade-off of DUET-VLM (C). Compared to LLaVA-1.5-7B, DUET-VLM (C) reduces training time by 26%, 31%, and 36% at 192, 128, and 64 tokens, respectively, while maintaining 99.7% and 99.1% average accuracy at 192 and 128 tokens. Even under aggressive compression (64 tokens), the model preserves 95.4% of baseline accuracy, confirming that DUET provides a favorable training efficiency-accuracy balance.

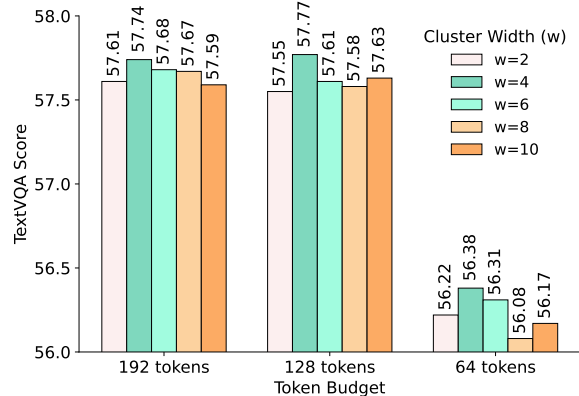


Figure 3. Ablation on varying cluster width of DUET-VLM (C) on VQA^T benchmark on LLaVA-1.5-7B for different token budgets.

Inference-Only Results on Video-LLaVA-7B. Table 4 presents results on the Video-LLaVA-7B model evaluated across TGIF [10], MSVD [29], and MSRVTT [29] benchmarks under two different token budgets. The full model processes 2048 vision tokens as the upper bound, while our DUET-VLM (C) and other baselines are evaluated at 960 (53.1% reduction) and 136 (93.4% reduction) tokens. At 960 tokens, DUET-VLM (C) achieves an average accuracy of 100.8%, even slightly surpassing the baseline, demonstrating that our compression retains or enhances task-relevant representations. At extreme compression (136 tokens), DUET-VLM (C) still maintains 97.6% of the full-model performance, substantially outperforming FastV [5], SparseVLM [34], and VisionZip by large margins (over 15% on average). These results highlight that video sequences contain significant temporal redundancy and that our proposed dual-compression strategy preserves essential

cross-frame information while removing redundant content. Overall, DUET-VLM achieves superior efficiency without compromising multimodal reasoning or video understanding accuracy.

Table 7. Comparison showing benefits of our local cluster aggregation on LLaVA-1.5-7B across 6 benchmarks. We report numbers for different methods (M): LLaVA-1.5-7B (Base), Vanilla (V), VisionZip (VZ), VisionZip with our proposed clustering (VZ (C)), and DUET-VLM (Vanilla) (DV (V)) variants defined in Sec. 4.1

M	POPE	SQA ^I	VQA ^T	MME	GQA	Seed ^I	Avg
Total 576 Tokens (100.0%)							
Base	85.9	69.5	58.2	1862	61.9	66.1	100.0%
Avg 192 Tokens (↓ 66.7%)							
VZ	85.3	68.9	57.3	1783	59.3	59.9	96.5%
VZ (C)	85.8	68.6	57.6	1743	59.0	63.4	97.1%
DV (V)	85.6	68.2	55.0	1802	58.8	64.6	97.0%
(C)	86.5	69.6	57.7	1817	60.3	65.1	98.9%
Avg 128 Tokens (↓ 77.8%)							
VZ	83.2	68.9	56.8	1762	57.6	58.0	94.8%
VZ (C)	83.4	68.5	57.1	1748	57.6	61.7	95.7%
DV (V)	83.9	69.5	51.8	1679	58.1	60.0	93.6%
(C)	85.9	70.2	57.8	1767	59.0	63.5	97.8%
Avg 64 Tokens (↓ 88.9%)							
VZ	77.0	69.0	55.5	1690	55.1	55.2	91.3%
VZ (C)	76.9	69.4	55.5	1706	55.4	57.6	92.2%
DV (V)	77.8	67.9	48.3	1565	55.5	56.4	88.4%
(C)	82.5	68.3	56.4	1751	56.7	60.7	94.8%

4.3. Ablations

Effect of Local Clustering on LLaVA Models. Table 7 evaluates our local clustering mechanism on LLaVA-1.5-7B. Across all token budgets, DUET-VLM (C) consistently surpasses VisionZip, DUET-VLM (Vanilla), and even VisionZip (C)—shows clear gains over the original VisionZip demonstrating the general utility of local neighborhood aggregation. As shown in Figure 3, varying cluster width ($\{4:6\}$) yield the best TextVQA [24] performance by balancing preservation and redundancy reduction. as smaller or larger clusters cause, either over-fragmentation or over-smoothing. Overall, DUET-VLM (C) achieves up to 97.1% of baseline accuracy under heavy compression, validating that localized clustering is key to compact yet semantically rich token representation.

Effect of Text-Guided Token Selection in DUET-VLM. Tables 8 and 9 present an ablation for different token selection strategies within the language backbone of DUET-VLM for both LLaVA-1.5-7B and LLaVA-NeXT-7B. For both models and all token budgets, DUET-VLM (C+S) consistently

Table 8. Comparison of DUET-VLM on LLaVA-1.5-7B under different text token selection schemes for language model-side pruning. We evaluate different Methods (M): LLaVA-1.5-7B (Base) and our clustering-based variants defined in Sec. 4.1 across different benchmarks. DUET-VLM maintains strong accuracy even with up to 88.9% fewer tokens highlighting the effectiveness of our dual-stage visual token compression.

M	POPE	SQA ^I	VQA ^T	MME	GQA	Seed ^I	Avg
Total 576 Tokens (100.0%)							
Base	85.9	69.5	58.2	1862	61.9	66.1	100.0%
Avg 192 Tokens (↓ 66.7%)							
(C)	86.5	69.6	57.7	1817	60.3	65.1	98.9%
(C+all)	86.4	68.2	57.8	1813	60.2	65.1	98.5%
(C+S)	86.4	68.2	57.7	1823	60.2	65.1	98.6%
Avg 128 Tokens (↓ 77.8%)							
(C)	85.9	70.2	57.8	1767	59.0	63.5	97.8%
(C+all)	85.9	68.4	57.8	1763	59.1	63.5	97.3%
(C+S)	85.9	68.4	57.7	1763	59.0	63.6	97.3%
Avg 64 Tokens (↓ 88.9%)							
(C)	82.5	68.3	56.4	1751	56.7	60.7	94.8%
(C+all)	82.5	68.3	56.3	1753	56.6	60.7	94.7%
(C+S)	82.5	68.3	56.2	1757	56.6	60.7	94.8%

Table 9. Comparison of DUET-VLM on LLaVA-NeXT-7B under different text token selection schemes for language model-side pruning. We evaluate different methods (M): LLaVA-NeXT-7B (Base), and our clustering-based variants defined in Sec. 4.1. DUET-VLM maintains strong accuracy >91% even at 94.4% reduction in tokens.

M	POPE	SQA ^I	VQA ^T	MME	GQA	Seed ^I	Avg
Upper Bound, 2880 Tokens (100.0%)							
Base	86.4	70.2	61.3	1842	64.2	70.2	100.0%
Avg 640 Tokens (↓ 77.8%)							
(C)	87.2	68.4	59.5	1839	61.8	68.5	98.2%
(C+all)	87.2	68.5	59.4	1840	61.7	68.5	98.2%
(C+S)	87.2	68.5	59.5	1839	61.6	68.5	98.2%
Avg 320 Tokens (↓ 88.9%)							
(C)	85.0	67.5	58.0	1771	60.1	65.6	95.4%
(C+all)	85.1	67.0	57.8	1772	60.2	65.7	95.3%
(C+S)	85.0	67.1	57.9	1772	60.2	65.7	95.3%
Avg 160 Tokens (↓ 94.4%)							
(C)	80.5	67.6	57.0	1672	57.6	61.6	91.8%
(C+all)	80.5	67.8	56.4	1670	57.6	61.6	91.6%
(C+S)	80.6	67.6	56.7	1670	57.6	61.6	91.7%

performs on par with or better than the other variants, particularly at higher compression levels. For instance, on LLaVA-1.5-7B, DUET-VLM (C+S) achieves 98.9%, 97.8%, and 94.8% of baseline accuracy at 192, 128, and 64 tokens, re-



Figure 4. Attention heatmap of salient text tokens attending to visual tokens at the 9th layer of the language backbone in DUET-VLM (C+S).

spectively, showing strong retention even with 89% token reduction. Similarly, on LLaVA-NeXT-7B, the (C+S) variant attains 98.2%, 95.4%, and 91.7% accuracy at 640, 320, and 160 tokens, respectively, matching or slightly exceeding the (C+all) configuration across all benchmarks. The advantage of (C+S) lies in its ‘selective focus’: salient text tokens provide sharper contextual cues for identifying relevant visual regions, avoiding the over-smoothing effect introduced when all text tokens are used equally. This targeted text guidance enhances token importance estimation, allowing the model to preserve semantically rich patches while pruning redundant ones more effectively. These results validate that coupling text-guided saliency with visual clustering is a key factor behind DUET-VLM’s superior efficiency–accuracy trade-off and represents one of the core contributions of this work.

Qualitative Analysis. From the attention heatmap in Fig. 4, we observe that the salient text tokens (including the last text token) guide the token-dropping mechanism in DUET-VLM, narrowing the model’s focus toward query-relevant image regions. This selective emphasis helps remove irrelevant background and distracting objects, leading to more accurate visual reasoning.

5. Conclusion

In this work, we introduced DUET-VLM, a dual-stage visual compression framework that achieves efficient and accurate multimodal learning under aggressive token reduction. Our key insight is that redundancy exists both spatially in vision tokens and contextually during multimodal fusion. By combining redundancy-aware visual token merging in the vision encoder with saliency-based text-guided token pruning in the language backbone, DUET-VLM achieves substantial compression while retaining semantically critical information. Experiments on image and video benchmarks show that DUET-VLM maintains near-baseline accuracy in inference-only settings and even surpasses baseline performance when fine-tuned under the same compression regime across all benchmarks. These findings demonstrate that training-aware token management—not model scaling—is a promising path toward compact yet high-performing VLMs. A comprehensive sensitivity analysis of parameters k_1 , k_2 , λ , and l is provided in the supplemental. We do not report exact infer-

ence or training times, but our runtimes are comparable to VisionZip [30] under the same token budget.

A detailed speed analysis is left for future work, as we aim to develop optimized kernels to further accelerate both inference and training. We also leave the training of video models and inference on longer-horizon videos (with more frames than our current setting) to future work, enabled by the minimal accuracy drop observed even under extreme token compression with our approach. For more precise visual token reduction in vision encoder, future work may explore stronger region-proposal or saliency-based methods beyond the current V2V self-attention filtering. Finally, we would like to extend this dual-stage vision compression paradigm to additional modalities (*e.g.*, audio and text) and further advance practical, scalable multimodal systems.

References

- [1] Kazi Hasan Ibn Arif, JinYi Yoon, Dimitrios S Nikolopoulos, Hans Vandierendonck, Deepu John, and Bo Ji. HiRED: Attention-Guided Token Dropping for Efficient Inference of High-Resolution Vision-Language Models. In *Association for the Advancement of Artificial Intelligence (AAAI)*, 2025. 2, 5
- [2] Jinze Bai, Shuai Bai, Yunfei Chu, Zeyu Cui, Kai Dang, Xiaodong Deng, Yang Fan, Wenbin Ge, Yu Han, Fei Huang, et al. Qwen technical report. *arXiv preprint arXiv:2309.16609*, 2023. 2
- [3] Shuai Bai, Keqin Chen, Xuejing Liu, Jialin Wang, Wenbin Ge, Sibao Song, Kai Dang, Peng Wang, Shijie Wang, Jun Tang, Humen Zhong, Yanzhi Zhu, Mingkun Yang, Zhaohai Li, Jianqiang Wan, Pengfei Wang, Wei Ding, Zheren Fu, Yiheng Xu, Jiabo Ye, Xi Zhang, Tianbao Xie, Zesen Cheng, Hang Zhang, Zhibo Yang, Haiyang Xu, and Junyang Lin. Qwen2.5-vl technical report, 2025. 6
- [4] Jun Chen, Deyao Zhu, Xiaoqian Shen, Xiang Li, Zechu Liu, Pengchuan Zhang, Raghuraman Krishnamoorthi, Vikas Chandra, Yunyang Xiong, and Mohamed Elhoseiny. MiniGPT-v2: large language model as a unified interface for vision-language multi-task learning. *arXiv preprint arXiv:2310.09478*, 2023. 2
- [5] Liang Chen, Haozhe Zhao, Tianyu Liu, Shuai Bai, Junyang Lin, Chang Zhou, and Baobao Chang. An Image is Worth 1/2 Tokens After Layer 2: Plug-and-Play Inference Acceleration for Large Vision-Language Models. In *European Conference on Computer Vision (ECCV)*, 2024. 2, 5, 7

- [6] Yukang Chen, Shengju Qian, Haotian Tang, Xin Lai, Zhi-jian Liu, Song Han, and Jiaya Jia. LongLoRA: Efficient Fine-tuning of Long-Context Large Language Models. In *International Conference on Learning Representations (ICLR)*, 2024. 2
- [7] Wei-Lin Chiang, Zhuohan Li, Zi Lin, Ying Sheng, Zhanghao Wu, Hao Zhang, Lianmin Zheng, Siyuan Zhuang, Yonghao Zhuang, Joseph E. Gonzalez, Ion Stoica, and Eric P. Xing. Vicuna: An Open-Source Chatbot Impressing GPT-4 with 90%* ChatGPT Quality, 2023. 2
- [8] Wenliang Dai, Junnan Li, Dongxu Li, Anthony Meng Huat Tiong, Junqi Zhao, Weisheng Wang, Boyang Li, Pascale Fung, and Steven Hoi. InstructBLIP: towards general-purpose vision-language models with instruction tuning. In *Advances in Neural Information Processing Systems (NeurIPS)*, 2023. 2
- [9] Drew A Hudson and Christopher D Manning. GQA: A New Dataset for Real-World Visual Reasoning and Compositional Question Answering. In *Conference on Computer Vision and Pattern Recognition (CVPR)*, 2019. 4, 7
- [10] Yunseok Jang, Yale Song, Youngjae Yu, Youngjin Kim, and Gunhee Kim. TGIF-QA: Toward Spatio-Temporal Reasoning in Visual Question Answering. In *Conference on Computer Vision and Pattern Recognition (CVPR)*, 2017. 4, 7
- [11] Sehoon Kim, Sheng Shen, David Thorsley, Amir Gholami, Woosuk Kwon, Joseph Hassoun, and Kurt Keutzer. Learned Token Pruning for Transformers. In *ACM SIGKDD Conference on Knowledge Discovery and Data Mining (KDD)*, 2022. 2
- [12] Bohao Li, Rui Wang, Guangzhi Wang, Yuying Ge, Yixiao Ge, and Ying Shan. SEED-Bench: Benchmarking Multimodal LLMs with Generative Comprehension. In *Conference on Computer Vision and Pattern Recognition (CVPR)*, 2024. 4
- [13] Yifan Li, Yifan Du, Kun Zhou, Jinpeng Wang, Xin Zhao, and Ji-Rong Wen. Evaluating Object Hallucination in Large Vision-Language Models. In *Empirical Methods in Natural Language Processing (EMNLP)*, 2023. 4, 7
- [14] Yanwei Li, Yuechen Zhang, Chengyao Wang, Zhisheng Zhong, Yixin Chen, Ruihang Chu, Shaoteng Liu, and Jiaya Jia. Mini-Gemini: Mining the Potential of Multi-modality Vision Language Models. *arXiv:2403.18814*, 2023. 2
- [15] Bin Lin, Bin Zhu, Yang Ye, Munan Ning, Peng Jin, and Li Yuan. Video-LLaVA: Learning United Visual Representation by Alignment Before Projection. In *Empirical Methods in Natural Language Processing (EMNLP)*, 2024. 4
- [16] Haotian Liu, Chunyuan Li, Qingyang Wu, and Yong Jae Lee. Visual Instruction Tuning. In *Advances in Neural Information Processing Systems (NeurIPS)*, 2023. 1, 2
- [17] Haotian Liu, Chunyuan Li, Yuheng Li, and Yong Jae Lee. Improved Baselines with Visual Instruction Tuning. In *Conference on Computer Vision and Pattern Recognition (CVPR)*, 2024. 4, 6
- [18] Haotian Liu, Chunyuan Li, Yuheng Li, Bo Li, Yuanhan Zhang, Sheng Shen, and Yong Jae Lee. LLaVA-NeXT: Improved reasoning, OCR, and world knowledge, 2024. 1, 2, 4
- [19] Pan Lu, Swaroop Mishra, Tanglin Xia, Liang Qiu, Kai-Wei Chang, Song-Chun Zhu, Oyvind Tafjord, Peter Clark, and Ashwin Kalyan. Learn to Explain: Multimodal Reasoning via Thought Chains for Science Question Answering. *Advances in Neural Information Processing Systems (NeurIPS)*, 2022. 4
- [20] R OpenAI. Gpt-4 technical report. *View in Article*, 2(5):1, 2023. 2
- [21] Alec Radford, Jong Wook Kim, Chris Hallacy, Aditya Ramesh, Gabriel Goh, Sandhini Agarwal, Girish Sastry, Amanda Askell, Pamela Mishkin, Jack Clark, et al. Learning transferable visual models from natural language supervision. In *International Conference on Machine Learning (ICML)*. PMLR, 2021. 2
- [22] Rafael Rafailov, Archit Sharma, Eric Mitchell, Christopher D Manning, Stefano Ermon, and Chelsea Finn. Direct Preference Optimization: Your Language Model is Secretly a Reward Model. In *Advances in Neural Information Processing Systems (NeurIPS)*, 2023. 2
- [23] Yuzhang Shang, Mu Cai, Bingxin Xu, Yong Jae Lee, and Yan Yan. LLaVA-PruMerge: Adaptive Token Reduction for Efficient Large Multimodal Models. In *International Conference on Computer Vision (ICCV)*, 2025. 2, 5
- [24] Amanpreet Singh, Vivek Natarajan, Meet Shah, Yu Jiang, Xinlei Chen, Dhruv Batra, Devi Parikh, and Marcus Rohrbach. Towards VQA Models That Can Read. In *Conference on Computer Vision and Pattern Recognition (CVPR)*, 2019. 4, 8
- [25] Dingjie Song, Wenjun Wang, Shunian Chen, Xidong Wang, Michael X. Guan, and Benyou Wang. Less is More: A Simple yet Effective Token Reduction Method for Efficient Multimodal LLMs. In *International Conference on Computational Linguistics (COLING)*, 2025. 2
- [26] Shengbang Tong, Ellis Brown, Penghao Wu, Sanghyun Woo, Manoj Middepogu, Sai Charitha Akula, Jihan Yang, Shusheng Yang, Adithya Iyer, Xichen Pan, Austin Wang, Rob Fergus, Yann LeCun, and Saining Xie. Cambrian-1: a fully open, vision-centric exploration of multimodal LLMs. In *Advances in Neural Information Processing Systems (NeurIPS)*, 2025. 2
- [27] Hugo Touvron, Thibaut Lavril, Gautier Izacard, Xavier Martinet, Marie-Anne Lachaux, Timothée Lacroix, Baptiste Rozière, Naman Goyal, Eric Hambro, Faisal Azhar, et al. Llama: Open and efficient foundation language models. *arXiv preprint arXiv:2302.13971*, 2023. 2
- [28] Long Xing, Qidong Huang, Xiaoyi Dong, Jiajie Lu, Pan Zhang, Yuhang Zang, Yuhang Cao, Conghui He, Jiaqi Wang, Feng Wu, et al. Pyramidrop: Accelerating your large vision-language models via pyramid visual redundancy reduction. In *Conference on Computer Vision and Pattern Recognition (CVPR)*, 2025. 2, 3, 4, 5, 12
- [29] Dejing Xu, Zhou Zhao, Jun Xiao, Fei Wu, Hanwang Zhang, Xiangnan He, and Yueting Zhuang. Video question answering via gradually refined attention over appearance and motion. In *ACM Multimedia (MM)*, 2017. 4, 7
- [30] Senqiao Yang, Yukang Chen, Zhuotao Tian, Chengyao Wang, Jingyao Li, Bei Yu, and Jiaya Jia. VisionZip: Longer is Better but Not Necessary in Vision Language Models. In *Conference on Computer Vision and Pattern Recognition (CVPR)*, 2025. 2, 3, 5, 9

- [31] Weihao Ye, Qiong Wu, Wenhao Lin, and Yiyi Zhou. Fit and prune: Fast and training-free visual token pruning for multi-modal large language models. In *Association for the Advancement of Artificial Intelligence (AAAI)*, 2025. [2](#), [5](#)
- [32] Shukang Yin, Chaoyou Fu, Sirui Zhao, Ke Li, Xing Sun, Tong Xu, and Enhong Chen. A Survey on Multimodal Large Language Models. *National Science Review*, 11(12):nwae403, 2024. [4](#)
- [33] Xiaohua Zhai, Basil Mustafa, Alexander Kolesnikov, and Lucas Beyer. Sigmoid Loss for Language Image Pre-Training. In *International Conference on Computer Vision (ICCV)*, 2023. [2](#)
- [34] Yuan Zhang, Chun-Kai Fan, Junpeng Ma, Wenzhao Zheng, Tao Huang, Kuan Cheng, Denis Gudovskiy, Tomoyuki Okuno, Yohei Nakata, Kurt Keutzer, et al. SparseVLM: Visual Token Sparsification for Efficient Vision-Language Model Inference. In *International Conference on Learning Representations (ICLR)*, 2025. [5](#), [7](#)
- [35] Chuanyang Zheng, Yihang Gao, Han Shi, Minbin Huang, Jingyao Li, Jing Xiong, Xiaozhe Ren, Michael Ng, Xin Jiang, Zhenguo Li, and Yu Li. DAPE: Data-Adaptive Positional Encoding for Length Extrapolation. In *Advances in Neural Information Processing Systems (NeurIPS)*, 2024. [2](#)
- [36] Deyao Zhu, Jun Chen, Xiaoqian Shen, Xiang Li, and Mohamed Elhoseiny. MiniGPT-4: Enhancing Vision-Language Understanding with Advanced Large Language Models. *arXiv preprint arXiv:2304.10592*, 2023. [2](#)

A. Sensitivity Analysis

Effect on varying parameters λ and l . To study the behavior of our token-dropping mechanism, we analyze the effect of the compression ratio λ and the stage index l in Fig. 5. Here, $\lambda \in [0, 1]$ denotes the fraction of vision tokens dropped at each stage, and $l \in \{1, 2, 3\}$ indexes the segmentation stages of the language backbone. In all experiments, we fix the three segmentation points at [8, 16, 24] layers, corresponding to the three stages, and vary λ to evaluate the sensitivity of our method. We observe that pruning tokens entirely in the final layers has only a minimal effect on performance. The red crosses denote configurations in which all vision tokens are pruned starting in one of three stages. When this 100% pruning occurs in the middle stage, i.e., where $\lambda = 0$ for all layers after the 16th layer performance degrades because the visual information has not yet been fully extracted into the hidden states. However, in the later layers (last stage), this information has already been extracted, making the vision tokens redundant. Consequently, for all configurations where 100% pruning occurs after the 24th layer, the performance remains competitive. A simple visualization of this can be seen in Fig. 6 where at the 24th layer all the salient tokens as well as the last token focus on the required region, which implies that the required knowledge of the image has been transferred to the hidden states and the vision tokens are now redundant. We follow the 8-layer segmentation used in PyramidDrop [28] for this analysis. A more fine-grained, layer-by-layer investigation is left for future work.

Effect on varying parameters k_1 and k_2 . We analyze the effect of varying the number of dominant (k_1) and contextual (k_2) tokens across different cluster widths for a couple of token budgets as shown in Fig. 7 and Fig. 8 respectively. Since $k_1 + k_2$ is fixed by the token budget, we visualize only the variation in k_1 ; the corresponding trend for k_2 would be a symmetric reflection. Interestingly, the trends in Fig. 6 and Fig. 7 are not identical, and this difference directly informed our configuration choices. In Fig. 7 (192-token budget), we observe a clear upward trend as the number of dominant tokens k_1 increases toward the maximum feasible value (≈ 300), performance improves consistently across all cluster widths. This indicates that, at a relatively relaxed token budget, the model benefits from allocating a large dominant token pool, as it preserves more high-saliency visual information. However, in Fig. 8 (128-token budget), the trend changes. Here, performance peaks at a mid-range of dominant tokens (around 155–165) and then drops when k_1 becomes too large. This suggests that at stricter budgets, dominating the token set with high-saliency visual tokens (k_1) reduces contextual diversity and harms reasoning performance. Together, these results show that:

- At higher budgets (192 tokens) \rightarrow more dominant tokens

(k_1) are consistently better.

- At lower budgets (128 tokens) \rightarrow an intermediate dominant–contextual ($k_1 - k_2$) split yields the optimal balance. These observations guided our chosen configurations, we scale k_1 upward for larger budgets, while adopting a balanced dominant-contextual ratio ($k_1 : k_2$) for more aggressive compression scenarios.

B. Additional Experiments

Table 10. Comparison showing benefits of our local cluster aggregation on LLaVA-NeXT-7B across 6 benchmarks. We report numbers for different methods (M): LLaVA-NeXT-7B (Base), Vanilla (V), VisionZip (VZ), VisionZip with our proposed clustering (VZ (C)), DUET-VLM (Vanilla) (DV (V)) and our proposed method, DUET-VLM (C) represented as (C)

M	POPE	SQA ^I	VQA ^T	MME	GQA	Seed ^I	Avg
Upper Bound, 2880 Tokens (100%)							
V	86.4	70.2	61.3	1842	64.2	70.2	100.0%
Avg 640 Tokens (↓ 77.8%)							
VZ	86.3	68.1	60.2	1787	61.3	66.7	97.1%
VZ (C)	86.4	67.8	60.1	1786	61.3	66.9	97.1%
DV (V)	85.0	67.8	50.3	1750	60.7	65.8	93.4%
(C)	87.2	68.4	59.5	1839.0	61.8	68.5	98.2%
Avg 320 Tokens (↓ 88.9%)							
VZ	82.1	67.3	58.9	1702	59.3	63.4	93.7%
VZ (C)	82.1	67.4	59.1	1670	59.1	63.5	93.4%
DV (V)	80.6	68.2	47.0	1612	59.1	63.2	89.5%
(C)	85.0	67.5	58.0	1771	60.1	65.6	95.4%
Avg 160 Tokens (↓ 94.4%)							
VZ	74.8	68.3	56.2	1630	55.5	58.3	88.9%
VZ (C)	75.1	67.4	56.2	1650	54.9	58.3	88.8%
DV (V)	75.2	68.4	44.7	1576	57.8	61.4	86.7%
(C)	80.5	67.6	57.0	1672	57.6	61.6	91.8%

Table 11. Comparison of various token-selection schemes applied to PyramidDrop (PDrop) on top of LLaVA-1.5-7B (Base)

Method	VQA ^T	POPE	SQA ^I	MME	Avg
Total 576 Tokens (100%)					
Base	58.2	85.9	69.5	1862	100.0%
Avg 270 Tokens (↓ 53.1%)					
PDrop	57.5	84.8	69.4	1854.0	99.2%
PDrop (S)	57.6	85.2	69.2	1862	99.4%
PDrop (all)	57.8	85.2	69.2	1862.0	99.5%

Effect of local clustering on LLaVA-NeXT-7B. Across all token budgets, we consistently observe that local clustering

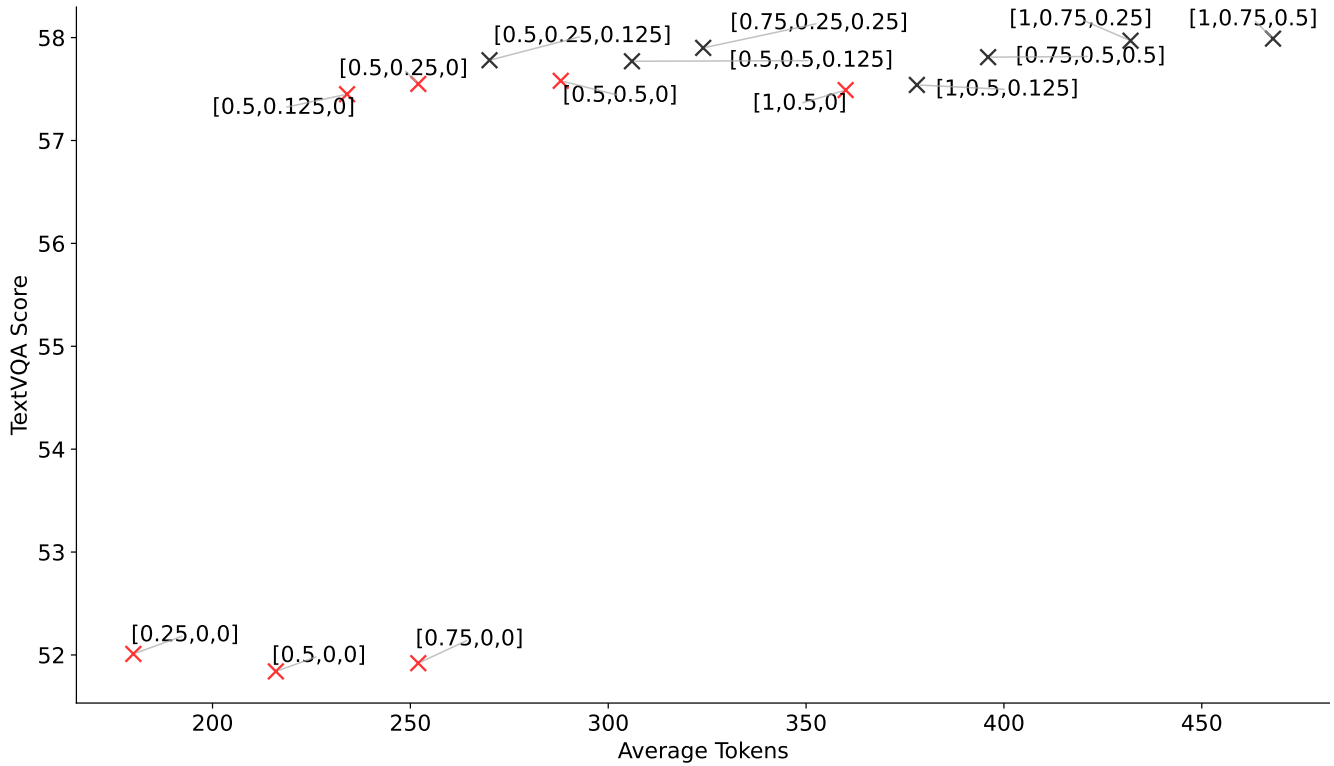


Figure 5. Performance of various dropping configurations in the language backbone on TextVQA using all text tokens. Red crosses indicate configurations in which all visual tokens are removed at some layer prior to the final layer.



Figure 6. Attention heatmap of salient text tokens attending to visual tokens at the 24th layer of the language backbone in DUET-VLM (C+S).

strengthens the performance of both VisionZip (VZ) and DUET-VLM (DV), demonstrating its robustness as a plug-in compression strategy. At the 640-token budget (78% reduction), clustering provides a modest yet stable improvement, indicating that early-stage redundancy is already substantial and can be effectively leveraged. As the budget becomes more restrictive (320 and 160 tokens), the benefit of clustering becomes even more pronounced: VisionZip (C) and DUET-VLM (C) retain significantly higher accuracy compared to their non-clustered counterparts, with DUET-VLM (C) showing the strongest resilience in the extremely low-token regime. This trend highlights that preservation of local structure is especially crucial when aggressively com-

pressing vision features allowing the model to retain the most semantically coherent groups of tokens rather than isolated high-scoring ones. Overall, the results confirm that local clustering provides a consistent, compression-aware advantage that amplifies the effectiveness of both VisionZip and DUET-VLM, particularly under severe token constraints.

Effect of Text Token Selection in PyramidDrop. Table 11 compares different strategies for selecting text tokens used to guide visual token ranking and pruning within PyramidDrop. The baseline approach of PyramidDrop relies on the *last text token* for ranking, while we propose two alternatives: *salient text tokens* (those with the highest attention

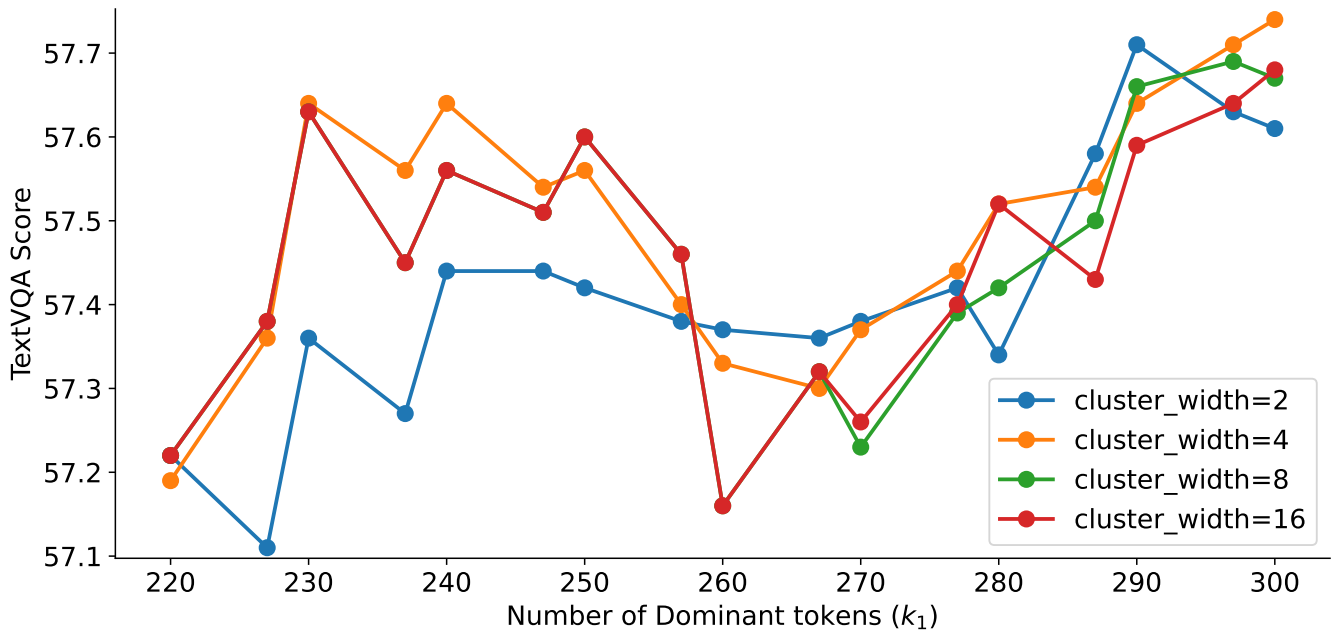


Figure 7. Plot of TextVQA performance across varying k_1 for different cluster widths, under the constraint $k_1 + k_2 = 307$ needed to meet a token budget of 192 using DUET-VLM (C) on LLaVA-1.5-7B.

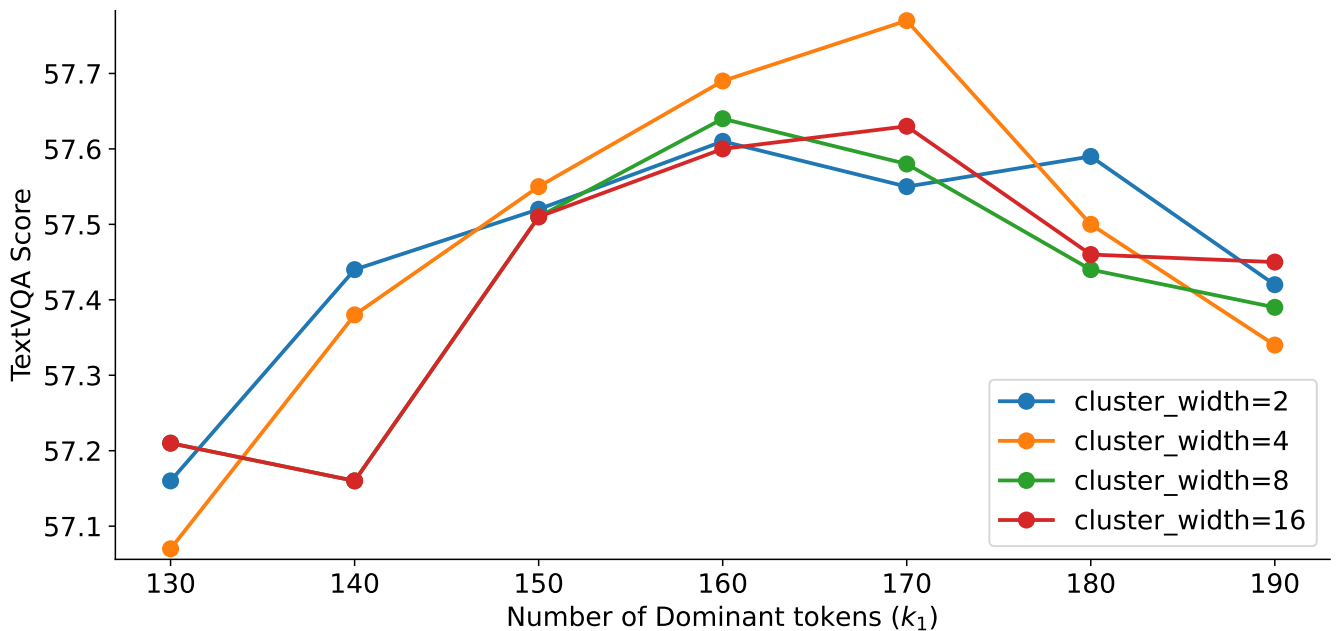


Figure 8. Plot of TextVQA performance across varying k_1 for different cluster widths, under the constraint $k_1 + k_2 = 205$ needed to meet a token budget of 128 using DUET-VLM (C) on LLaVA-1.5-7B.

weights) and *all query text tokens*. Both variants yield consistent improvement in accuracy across different benchmarks, demonstrating that leveraging broader and more relevant textual context enhances the model’s ability to estimate token importance and retain semantically relevant visual features.

Using all query tokens achieves the highest average accuracy (99.5%), marginally outperforming the salient-token variant (99.4%), suggesting that distributing attention across the full text sequence can better capture fine-grained multimodal relationships. Although the performance gap between the two

strategies is minimal, these findings confirm that integrating textual guidance into the ranking mechanism improves information retention without incurring additional computational cost.

C. Hyperparameters

Table 12. Vision token configuration used in the local clustering method for LLaVA-1.5-7B to achieve different target tokens

Target Tokens	Dominant	Contextual
192	300	7
128	170	35
64	72	30

Table 13. Vision token configuration used in the local clustering for LLaVA-NeXT-7B to achieve different target tokens

Target Tokens	Dominant	Contextual
640	850	175
320	360	150
160	225	30

Table 14. Vision token configuration used in the local clustering for Video-LLaVA-7B to achieve different target tokens

Target Tokens	Dominant	Contextual
960	1280	256
136	160	56

Token Numbers for Local Clustering. Tab. 12 reports the counts of dominant and contextual tokens selected for LLaVA-1.5-7B to meet three target token budgets after pruning on the language backbone side. Similarly, Tab. 13 presents these counts for LLaVA-NeXT-7B across three configurations. Tab. 14 summarizes the dominant and contextual token counts for Video-LLaVA-7B, which processes eight video frames to capture temporal context. These configurations are guided by the trends in Fig. 7 and Fig. 8, where higher token budgets favor the allocation of more dominant tokens, while tighter budgets achieve the best performance with a balanced dominant–contextual split.

Target Tokens	Dominant	Contextual
640	870	153
320	517	91
160	207	36

Table 15. Vision token configuration used in local clustering for Qwen2.5-VL-7B to achieve different target token budgets. The LLM-side rank-and-drop uses `layer_list = [14, 21]` and `image_token_ratio_list = [0.5, 0.25]`.